

## Surface-Guided Formation of an Organocobalt Complex

Peter B. Weber, Raphael Hellwig, Tobias Paintner, Marie Lattelais, Mateusz Paszkiewicz, Pablo Casado Aguilar, Peter S. Deimel, Yuanyuan Guo, Yi-Qi Zhang, Francesco Allegretti, Anthoula C. Papageorgiou, Joachim Reichert, Svetlana Klyatskaya, Mario Ruben, Johannes V. Barth, Marie-Laure Bocquet,\* and Florian Klappenberger\*

**Abstract:** Organocobalt complexes represent a versatile tool in organic synthesis as they are important intermediates in Pauson–Khand, Friedel–Crafts, and Nicholas reactions. Herein, a single-molecule-level investigation addressing the formation of an organocobalt complex at a solid–vacuum interface is reported. Deposition of 4,4'-(ethyne-1,2-diyl)dibenzonitrile and Co atoms on the Ag(111) surface followed by annealing resulted in genuine complexes in which single Co atoms laterally coordinated to two carbonitrile groups undergo organometallic bonding with the internal alkyne moiety of adjacent molecules. Alternative complexation scenarios involving fragmentation of the precursor were ruled out by complementary X-ray photoelectron spectroscopy. According to density functional theory analysis, the complexation with the alkyne moiety follows the Dewar–Chatt–Duncanson model for a two-electron-donor ligand where an alkyne-to-Co donation occurs together with a strong metal-to-alkyne back-donation.

Organocobalt complexes are a key reagent in organic synthesis because they can be used as a versatile tool for various reactions. In an industrial context these complexes are central in the multimillion-dollar technology of hydroformylation.<sup>[1]</sup> Furthermore, they are involved in various classic synthetic concepts, such as the Pauson–Khand<sup>[2]</sup> or the Nicholas<sup>[3]</sup> reactions. Amongst the most successful and popular compounds are dicobalt hexacarbonyls activating alkyne triple bonds by formation of a  $\mu^2$ -alkyne bridging the

Co–Co bond.<sup>[4]</sup> This important catalytic intermediate acts as a promoter for the Friedel–Crafts acylation<sup>[5]</sup> and mediates the [2+2+1] co-cyclization, known as the Pauson–Khand reaction.<sup>[2,6]</sup> The closely related cobalt-complexed propargyl cations are central ingredients in the Nicholas reaction.<sup>[3]</sup>

The exploration of metal–ligand interactions at well-defined surfaces presents an important alternative approach complementing classic solution-based synthetic procedures.<sup>[7]</sup> This strategy not only provides deep insight into the underlying mechanisms at the single-molecule level by rendering possible the application of surface-science techniques,<sup>[8]</sup> but also triggers the emergence of novel complexation phenomena unique to two-dimensional environments.<sup>[9]</sup> Notably, a series of metal–organic coordination networks were created, opening up prospects towards new functional surfaces with technological potential in a variety of fields and applications, such as host–guest chemistry,<sup>[10]</sup> catalysis,<sup>[11]</sup> and molecular nanomagnetism.<sup>[12]</sup>

Herein we employ the so-called STM + XS approach<sup>[8b]</sup> combining scanning tunneling microscopy (STM) with X-ray spectroscopy (XS) to identify the formation of a novel organocobalt complex evolving under interfacial confinement and to elucidate its intricate nature. Our real-space molecular-level insight reveals that on the Ag(111) surface, a unique cobalt compound can be synthesized in which a single Co atom is coordinated to two carbonitrile moieties and an internal alkyne. By STM we identify a strong distortion of the alkyne-bonded species, contrasting its originally linear conformation, which results from the complexation-induced rehybridization. Complementary X-ray photoelectron spectroscopy (XPS) measurements establish the core-level signature of the complex phase. A thorough analysis of the bonding mechanism with density functional theory (DFT) unravels strong analogies to the Dewar–Chatt–Duncanson ligation model.<sup>[13]</sup> However, contrary to the known isocyano organocobalt complexes,<sup>[14]</sup> herein we observe a nitrogen-lone-pair-mediated coordination of the carbonitriles. Furthermore, we demonstrate the self-assembly of chains of complexes originating from the ditopic nature of the employed ligand molecules.

For our study we employed the de novo synthesized 4,4'-(ethyne-1,2-diyl)dibenzonitrile (DBNE), depicted in Scheme 1, consisting of two benzonitrile moieties connected through a central alkyne unit (for the synthetic details see the Synthesis Section in the Supporting Information). The length of the molecule, defined as the distance between the nitrogen atoms, measures 14.9 Å according to DFT calculations. In a first step, a sub-monolayer coverage of DBNE was

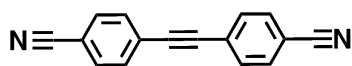
[\*] P. B. Weber, R. Hellwig, T. Paintner, M. Paszkiewicz, P. Casado Aguilar, P. S. Deimel, Dr. Y. Guo, Dr. Y.-Q. Zhang, Dr. F. Allegretti, Dr. A. C. Papageorgiou, Dr. J. Reichert, Prof. Dr. J. V. Barth, Dr. F. Klappenberger  
Physik Department E20, Technische Universität München  
James-Franck-Str., 85748 Garching (Germany)  
E-mail: florian.klappenberger@tum.de

Dr. M. Lattelais, Dr. M.-L. Bocquet  
Ecole Normale Supérieure, PSL Research University  
Département de Chimie, CNRS UMR  
8640 PASTEUR, 75005 Paris (France)  
E-mail: marie-laure.bocquet@ens.fr

Dr. S. Klyatskaya, Prof. Dr. M. Ruben  
Karlsruher Institut für Technologie  
Kaiserstraße 12, 76131 Karlsruhe (Germany)

Prof. Dr. M. Ruben  
IPCMS-CNRS, Université de Strasbourg  
23 rue de Loess, 67034 Strasbourg (France)

Supporting information for this article can be found under:  
<http://dx.doi.org/10.1002/anie.201600567>.



**Scheme 1.** Chemical structure of 4,4'-(ethyne-1,2-diyl)dibenzonitrile (DBNE).

evaporated onto the Ag(111) surface at 270 K followed by cooling and transfer to the microscope, where investigation took place at cryogenic temperature. We observed a regular molecular network (Figure 1a) dominating on the sample, whereby domains typically exhibit lateral dimensions as large as 500 nm. A superposition of scaled ball-and-stick models of DBNE onto a high-resolution image (Figure 1b) demonstrates a supramolecular packing with interdigitating, anti-parallel aligned CN groups and a distance of about 2 Å from terminal N atoms to the nearest hydrogen neighbor under the assumption of a completely planar conformation for the adsorbates. Similar self-assembly has been reported and thoroughly analyzed in previous work on carbonitrile-terminated species on the same substrate.<sup>[9f,15]</sup> Accordingly, we associate the observed pattern with dipole-dipole interactions between CN groups<sup>[16]</sup> and proton-acceptor ring interactions.<sup>[15e]</sup>

For exploring the metal-directed assembly, DBNE deposition followed by evaporation of Co atoms was carried out at a sample temperature of 135 K (see also the Supporting Information). In this case, an open-porous honeycomb-like network (Figure 1c) prevails on the surface. The network is

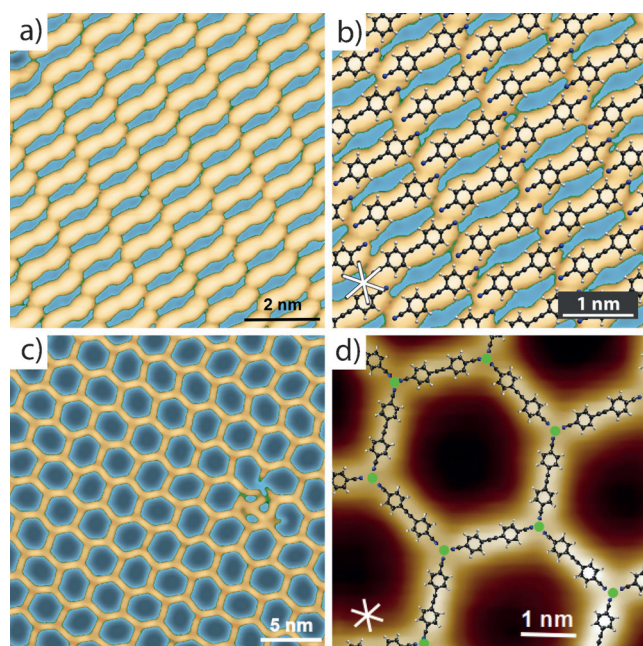


**Figure 1.** STM topographs of organic and metal-organic phases before complex formation. a) Dense packed network of DBNE molecules prior to Co deposition (bias voltage = 0.75 V, tunneling current = 65 pA). b) Expanded portion of (a) with overlaid molecular models. The distance between terminal N atoms and adjacent H atoms is approximately 2 Å. c) Metal-directed assembly of an open network after Co deposition at 135 K (−0.03 V, 30 pA). d) Expanded view of (c) with superimposed models of Co (green) and DBNE (−1.1 V, 0.305 nA).

explained by three-fold Co coordination, in analogy to earlier work with related, carbonitrile-terminated linker species.<sup>[9b,15c,17]</sup> In contrast to the previous studies in which highly crystalline arrangements with translational symmetry were observed, here the honeycomb network exhibits varying pore shapes. A simple analysis of large domains employing ball-and-stick models (Figure 1d) and assuming a strictly hexagonal geometry yields an unreasonably small Co–N binding distance of 1.0 Å. We conclude that the introduction of the central alkyne unit results in unfavorable epitaxy with respect to the underlying silver surface. Accordingly, the network adapts its geometry by deviations from the perfect six-fold symmetry, apparently facilitated by the increased flexibility provided by the carbon-carbon triple bond as compared to a purely phenylene backbone. Recent reports showed similar adaptive coordination networks constructed from linkers featuring a central butadiyne moiety.<sup>[18]</sup>

Following mild annealing to 250 K, the network transformed into a different phase (Figure 2a), where the pores appear elongated and line up in rows that are separated by zigzag-shaped double lines. This change results from the formation of a novel scissor-like structural motif (dashed lines) beside the three-fold coordination nodes (green with black lines). Further annealing to 350 K drives the formation of large domains entirely consisting of zigzag-shaped lines (Figure 2b) and areas of bare metal surface (not shown) where no residual porous structures persist. Figure 2c, showing an expanded portion of Figure 2b, demonstrates that the regular zigzag lines incorporate exclusively the scissor-like

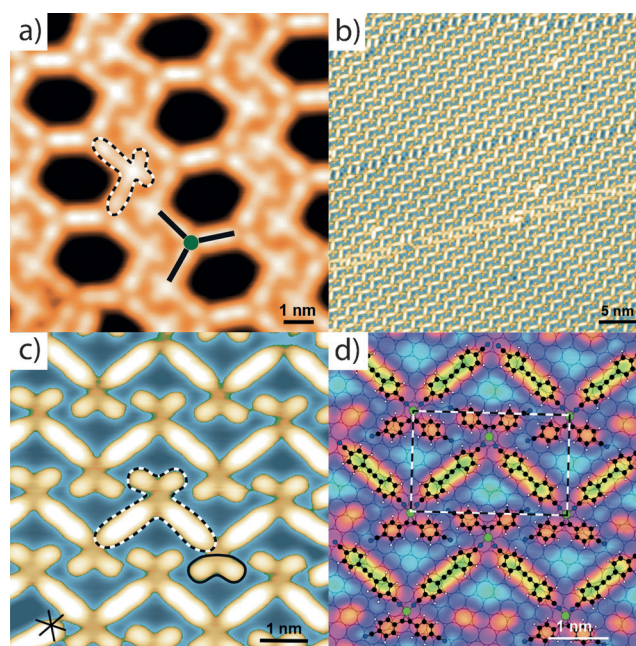


**Figure 2.** a) STM topograph of mixed-phase network (−0.3 V, 30 pA) obtained after mild annealing to 250 K. b, c) STM topographs of the complex network (0.32 V, 47 pA) obtained after further annealing to 350 K. In (c) a distorted DBNE is marked with a solid black line whereas the new scissor-shaped complex is outlined by the dashed black line. d) Schematic models of complexes superimposed on an STM topograph. The unit cell is indicated with a dashed outline.

motif (dashed line). This high-resolution version of the STM image allows us to clearly identify that this structure contains two bright and straight protrusions joined through a darker bridge to a curved feature (indicated with a black solid line). The curved protrusions suggest that a significant chemical change occurred for a portion of the molecules, which now adopt a modified, significantly bent conformation. The absence of Co clusters on the entire surface implies that the transition-metal atoms are involved in the scissor-shaped motifs. Accordingly, a qualitative model for the motif can be put forward suggesting a Co center surrounded by two straight and one strongly distorted unit of DBNE connected through the carbonitrile and alkyne groups, respectively (Figure 2d).

To better assess the chemical nature of the scissor motif we carried out XPS measurements (see the Supporting Information) in which we compared the three phases, namely the purely organic phase, the metal–organic phase, and the novel phase tentatively assigned to the organometallic complex motif. From the detected N 1s core-level signatures (see Figure S1 in the Supporting Information) we conclude that the metal–organic structure is indeed stabilized by CN–Co coordination and that the scissor motif is chemically distinct from the metal–organic phase. Furthermore, the N 1s signature of the organometallic complex phase contains two chemically inequivalent nitrogen species consistent with the tentative assignment in Figure 2d. The well-defined XPS signature also rules out more dramatic reaction scenarios based on complete disruption of the C≡C triple bond (Figure S2). Finally, based on the Co 2p data (Figure S1h), the Co atom in the scissor motif adopts a quasi-neutral state close to Co<sup>0</sup> within the complex.

Next, an investigation of the thermal stability of the scissor motifs by a series of STM experiments carried out at room temperature (Figure S3) demonstrated the structural integrity at 300 K. Neither three-fold coordination nodes nor hexagonal pores were detected, corroborating that the bonding of the scissor motif is of a different nature and is stronger than the three-fold coordination. Annealing temperatures above 373 K restore the pristine metal surface, signaling that dissolution of the complexes allowing desorption of the individual parts is possible and suggesting an, at least partially, reversible character of the scissor motif.

To determine the chemical nature of the complexes (Figures 2b–d), we carried out extensive DFT calculations, whereby we optimized different potential coordination/covalent bonding schemes. Notably, the three configurations displayed in Figure 3 were considered. The DFT model of the first complex, M1 (Figure 3, top), assumes that two pristine DBNE molecules coordinate to the Co center through the N lone pair of the CN group and the third ligand is distorted and attached through the central alkyne unit. The second possibility M2 (Figure 3, middle) is inspired by the 5-membered ring intermediate of a Co-catalyzed [2+2+2] cycloaddition reaction<sup>[19]</sup> and represents a variation of M1 where two DBNE ligands are covalently linked by a C–C coupling reaction of the  $\alpha$ -carbon atoms of the CN groups, in addition to concomitant N coordination leading to a 1,2-diimine-like ligand. Finally, the third complex, M3 (Figure 3,

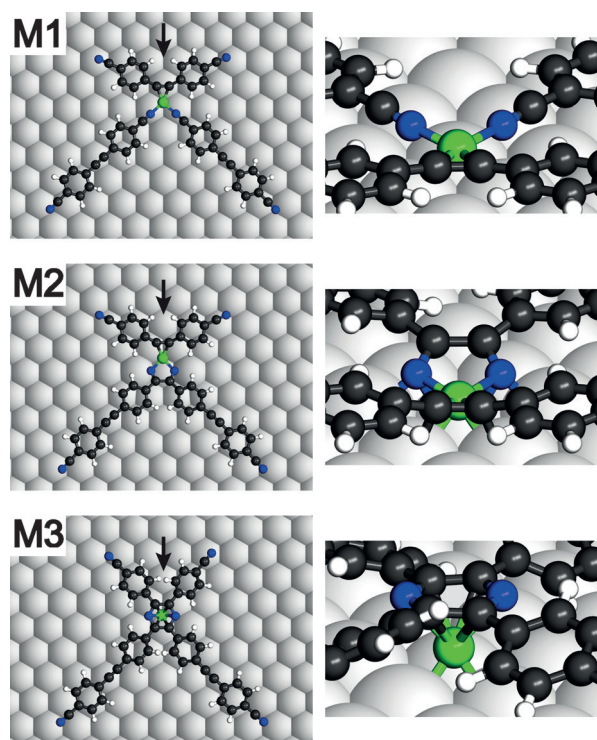


**Figure 3.** DFT-optimized models of complexes M1, M2, and M3 on the Ag(111) surface, showing the top (left panels) and side (right panels) views. Atom colors: Ag = gray; Co = green; C = black; N = blue; H = white. The side views are drawn assuming a direction-of-view as indicated by the arrows in the left panels and a glancing angle of 25°.

bottom), is inspired by the classical co-cyclization of triple bonds catalyzed by cobalt complexes: the two CN and alkyne units are cyclized through a [2+2+2] cycloaddition forming a pyrazine cycle. Here, the Co atom is situated below the center of the pyrazine between the substrate and the plane of the organic ring (see the side view in Figure 3, bottom) at a similar adsorption height as in the M2 case. In contrast, in the first model M1, the atom is pulled up from the surface and resides almost at the same height as the organic ligands. The Co heights above the surface (Ag atom centers) are 2.4 Å in M1, 1.7 Å for M2 and M3, and 1.6 Å for the isolated Co atoms.

The formation energies, that is, the energy of the combined system minus the energy of the individual constituents, of the different adsorbed complexes M1, M2, and M3 amount to  $-3.8$ ,  $-2.6$ , and  $-3.6$  eV, respectively. Thus, of the three possibilities, M1 seems energetically favorable. Interestingly, the energy balance of complex M3 comes close to that of M1, which results from the aromaticity of the formed six-membered ring. Note that these energies do not reflect the barriers of the transition states to be overcome during coupling and therefore neglect reaction kinetics.

To distinguish between the three models, the XPS signatures do not provide conclusive information. This results from the lack of reports on related complexes and the pyrazine N 1s binding energy being similar to that of the CN–Co type.<sup>[20]</sup> We focused instead on geometric considerations and carefully analyzed the structural characteristics of specific

configurations in nonperiodic structures (Figures S4, S5). The observed variety of the scissor motif opening angles is unlikely to appear for models M2 and M3 which feature covalently connected “blades”. Furthermore, the Co–Co distances in coordinated and complexed structures (see Figure S4) are equal within the experimental resolution and agree well with the length expected for intact DBNE coordinatively connecting Co atoms (see the Supporting Information), whereas significant structural disagreement well beyond the experimental error bar is detected for M2 and M3 (Figure S5).

Additional support for the reversible bonding nature behind the scissor motif is provided by manipulation experiments. We were able to induce a transformation from the asymmetric organocobalt complex (Figure S6a) to the three-fold symmetric coordination node (Figure S6b) by the combination of current pulses and movement of the STM tip. The reversible character is more likely to be compatible with the M1 configuration than with the covalent linking involved in M2 and M3.

To further substantiate our interpretation of the observed complexes according to model M1, simulated STM images were calculated of the three models and compared with the experimental topography data (Figure S7). The best agreement is obtained for model M1 (Figure 4).

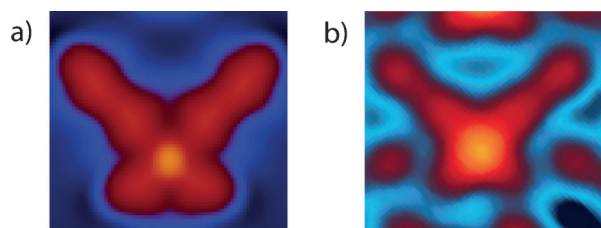


**Figure 4.** a) Simulated STM image of the complex at a bias voltage of  $-1$  V. b) Actual STM image of complex ( $-1$  V, 143 pA).

Considering these findings, we conclude that complex M1 is fully consistent with the combined experimental observations, including spectroscopic, structural, and electronic aspects.

Complex M1 can be interpreted in terms of the chemical structure shown in Figure 5a, in which formal conversion of the carbon–carbon triple bond into a double bond connected with the establishment of two carbon–cobalt bonds is assumed. Indeed, the DFT-calculated C–C bond lengths of the internal alkynes of the two intact DBNE (1.23 Å) and the distorted species (1.33 Å) assume values near those of prototypical triple and double bonds (1.20 Å for ethyne, 1.34 Å for ethene) and thus corroborate the suggested rehybridization. Indeed, similar organometallic bonding accompanied by carbon rehybridization in the vicinity of CO-coordinated Co centers is known for organocobalt complexes from solution chemistry.<sup>[21]</sup>

Various types of organocobalt-based catalysts exist involving combinations of oxygen- and nitrogen-coordinated Co centers.<sup>[1,22]</sup> Furthermore, cycloaddition reactions involving nitriles are known to proceed in the presence of cyclo-

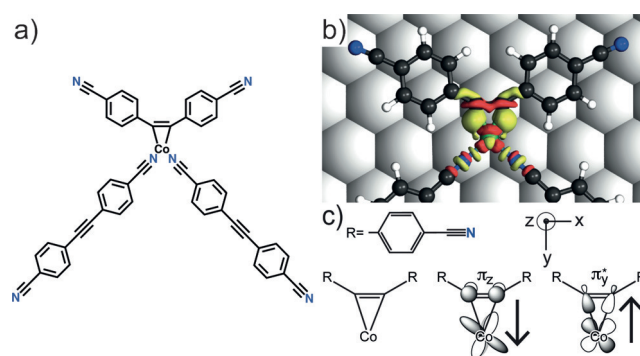


**Figure 5.** a) Chemical structure of complex M1. b) Charge-transfer map calculated from the difference between the charge density in the structure and the charge density of the isolated Co atom (the DBNE molecules and the Ag(111) surface are in the same position as in the composite structure). Red and yellow isosurfaces represent electron loss and gain, respectively, with absolute contour values of  $0.04 e_0 \text{ \AA}^{-3}$ . c) Schematic representation of the established Dewar–Chatt–Duncanson model for the Co–alkyne bonding: the metallacyclopropene (left) and presumed interactions characteristic of a  $2\pi$ -electron donor with  $\pi$ -donation (middle) and  $\pi$ -back-donation (right).

pentadienylcobalt complexes and related compounds.<sup>[1,23]</sup> Cyano cobalt catalysts, in which the CN moiety is connected to the cobalt center through the carbon atom, are widespread.<sup>[14,24]</sup> However, catalytic cobalt complexes with nitriles coordinated through the N lone pair are much more scarce. Complexes of this type have been reported in single-nitrile-coordinated compounds.<sup>[25]</sup> Because a twofold carbonitrile-coordinated organocobalt complex, as identified here, has not been previously reported, it is suggested that the underlying surface plays a crucial role in its formation.

The detailed DFT analysis of the electronic interaction provides further insights. Figure 5b shows the charge-transfer map calculated from the difference between the charge density of M1 and the charge densities of the isolated Co atom. The map displays spatial zones of electron gain (yellow) and electron loss (red) upon Co bonding to the molecular ligands on the Ag substrate. On the alkyne, there is clearly an electron depletion zone resembling one of the out-of-plane states of the alkynes along the  $z$  direction (see also the side view shown in Figure S8). The electron accumulation zone nearby mimics an in-plane state along the  $y$  direction. Furthermore, the electron loss of the in-plane d state ( $d_{xy}$ ) indicates electron back-donation. For interpreting the charge transfer, we combine molecular orbitals (MOs) of the Co center (d orbital manifold) with the alkyne MOs of matching symmetry (Figure 5c). These redistribution maps are in agreement with the MO interaction schemes given in Figure 5c. Classically, the metal–alkyne bonding in organocobalt complexes can be described by one resonance structure, specifically the metallacyclopropene shown in Figure 5c. The alkyne ligand has four  $\pi$ -electrons with two sets of occupied  $\pi$ -states and unoccupied  $\pi^*$ -states. The interaction with the Co atom follows the Dewar–Chatt–Duncanson model for a two-electron-donor ligand: an alkyne-to-Co electron donation with a strong metal-to-alkyne back-donation. The strong back-donation is characteristic of electron-

rich transition metals such as Co<sup>[26]</sup> and explains the occurrence of the metallocyclopropene form of the complex. In this form the alkyne is mostly hybridized to an alkene (sp<sup>2</sup> trigonal geometry) as a result of the weakening of one  $\pi$ -bond. This weakening originates from the back-donation process with electrons occupying one antibonding  $\pi^*$ -orbital of the alkyne.

In principle, even though not detected on the surface, an alternative complex structure where one Co center binds simultaneously to two ethynylene bridges can be hypothesized. To elucidate why the mixed complex M1 is preferred, we evaluated the binding energetics of two purely organometallic complexes in the gas phase, C1 and C2, and compared them with C3, the gas-phase variant of M1 (Figure S9). All three complexes were geometrically optimized without substrate. For C1, the alkyne ligands lie in the same plane and for C2 the alkynes are oriented perpendicular to each other. We find that the perpendicular structure is 1.2 eV more stable than the planar structure (total binding energy of -3.4 eV for C1 versus -4.6 eV for C2) in which the Co atom is displaced from the alkyne center, suggesting interfering steric repulsion between the phenyl groups. The stabilization of the perpendicular structure could be due to the favorable interactions between one triple C $\equiv$ C bond and the d<sub>xz</sub> orbital of Co and between the other triple C $\equiv$ C bond and the d<sub>yz</sub> orbital of Co. In comparison, the energy gained by the formation of C3 (5.6 eV) exceeds that of both purely organometallic complexes, which is consistent with the absence of complexes of C1 and C2 on the metallic surface.

In conclusion, our investigation demonstrates intricate organometallic complexation at well-defined surfaces under ultra-high-vacuum conditions, whereby novel complexes can be stabilized. Inspections at the single-molecule level combined with state-of-the-art theoretical modeling provide detailed insight into the pertaining structural and electronic properties. The reversible character of the bond formation, an essential property for its success as a catalytic intermediate in various synthetic pathways, is demonstrated by the ability to dissolve the metal-organic complexes with rather mild temperatures and molecular manipulation experiments. Furthermore, our results are equally important for the rapidly evolving field of on-surface covalent synthesis. This work will facilitate the expansion of the previously employed direct-coupling mechanisms using alkynes<sup>[27]</sup> to more sophisticated pathways via controlled catalytic reaction intermediates and transition-metal centers incorporated in specific environments.

## Acknowledgements

Funding was provided by the EU through the ERC Advanced Grant MolArt (Grant 247299), the Munich Center for Advanced Photonics, the TUM Institute of Advanced Study (IAS) funded by the German Excellence Initiative, and the German Research Foundation (DFG) through KL 2294/3-1. M.L., M.-L.B. and J.V.B. thank the collaborative transnational grant in the ANR-DFG 2011 call (ANR-11-INTB-1014-01) for support. Computer resources have been provided by the

Gauss Centre for Supercomputing/Leibniz Supercomputing Centre (Grant ID: pr851a) and the Pole Scientifique de Modélisation Numérique (PSMN) in ENS de Lyon.

**Keywords:** alkynes · density functional calculations · organocobalt complexes · scanning tunneling microscopy · surface chemistry

**How to cite:** *Angew. Chem. Int. Ed.* **2016**, *55*, 5754–5759

*Angew. Chem.* **2016**, *128*, 5848–5853

- [1] I. Omae, *Appl. Organomet. Chem.* **2007**, *21*, 318–344.
- [2] P. L. Pauson, *Tetrahedron* **1985**, *41*, 5855–5860.
- [3] K. M. Nicholas, *Acc. Chem. Res.* **1987**, *20*, 207–214.
- [4] W. G. Sly, *J. Am. Chem. Soc.* **1959**, *81*, 18–20.
- [5] D. Seyferth, A. T. Wehman, *J. Am. Chem. Soc.* **1970**, *92*, 5520–5522.
- [6] a) S. Laschat, A. Becheanu, T. Bell, A. Baro, *Synlett* **2005**, 2547–2570; b) K. M. Brummond, J. L. Kent, *Tetrahedron* **2000**, *56*, 3263–3283.
- [7] a) J. V. Barth, *Surf. Sci.* **2009**, *603*, 1533–1541; b) J. A. A. W. Elemans, S. B. Lei, S. De Feyter, *Angew. Chem. Int. Ed.* **2009**, *48*, 7298–7332; *Angew. Chem.* **2009**, *121*, 7434–7469; c) N. Lin, S. Stepanow, M. Ruben, J. V. Barth, *Top. Curr. Chem.* **2009**, *287*, 1–44.
- [8] a) S. M. Barlow, R. Raval, *Surf. Sci. Rep.* **2003**, *50*, 201–341; b) F. Klappenberger, *Prog. Surf. Sci.* **2014**, *89*, 1–55.
- [9] a) S. Stepanow, N. Lin, D. Payer, U. Schlickum, F. Klappenberger, G. Zoppellaro, M. Ruben, H. Brune, J. V. Barth, K. Kern, *Angew. Chem. Int. Ed.* **2007**, *46*, 710–713; *Angew. Chem.* **2007**, *119*, 724–727; b) U. Schlickum, R. Decker, F. Klappenberger, G. Zoppellaro, S. Klyatskaya, M. Ruben, I. Silanes, A. Arnau, K. Kern, H. Brune, J. V. Barth, *Nano Lett.* **2007**, *7*, 3813–3817; c) F. Cicoira, C. Santato, F. Rosei, *Top. Curr. Chem.* **2008**, *285*, 203–267; d) G. Pawin, K. L. Wong, D. Kim, D. Z. Sun, L. Bartels, S. Hong, T. S. Rahman, R. Carp, M. Marsella, *Angew. Chem. Int. Ed.* **2008**, *47*, 8442–8445; *Angew. Chem.* **2008**, *120*, 8570–8573; e) M. Marschall, J. Reichert, A. Weber-Bargioni, K. Seufert, W. Auwärter, S. Klyatskaya, G. Zoppellaro, M. Ruben, J. V. Barth, *Nat. Chem.* **2010**, *2*, 131–137; f) S. Klyatskaya, F. Klappenberger, U. Schlickum, D. Kühne, M. Marschall, J. Reichert, R. Decker, W. Krenner, G. Zoppellaro, H. Brune, J. V. Barth, M. Ruben, *Adv. Funct. Mater.* **2011**, *21*, 1230–1240; g) D. Écija, J. I. Urgel, A. C. Papageorgiou, S. Joshi, W. Auwärter, A. P. Seitsonen, S. Klyatskaya, M. Ruben, S. Fischer, S. Vijayaraghavan, J. Reichert, J. V. Barth, *Proc. Natl. Acad. Sci. USA* **2013**, *110*, 6678–6681; h) A. Shchyrba, C. Wäckerlin, J. Nowakowski, S. Nowakowska, J. Björk, S. Fatayer, J. Girovsky, T. Nijs, S. C. Martens, A. Kleibert, M. Stöhr, N. Ballav, T. A. Jung, L. H. Gade, *J. Am. Chem. Soc.* **2014**, *136*, 9355–9363.
- [10] S. Stepanow, M. Lingenfelder, A. Dmitriev, H. Spillmann, E. Delvigne, N. Lin, X. B. Deng, C. Z. Cai, J. V. Barth, K. Kern, *Nat. Mater.* **2004**, *3*, 229–233.
- [11] S. Fabris, S. Stepanow, N. Lin, P. Gambardella, A. Dmitriev, J. Honolka, S. Baroni, K. Kern, *Nano Lett.* **2011**, *11*, 5414–5420.
- [12] P. Gambardella, S. Stepanow, A. Dmitriev, J. Honolka, F. M. F. de Groot, M. Lingenfelder, S. Sen Gupta, D. D. Sarma, P. Bencok, S. Stanesco, S. Clair, S. Pons, N. Lin, A. P. Seitsonen, H. Brune, J. V. Barth, K. Kern, *Nat. Mater.* **2009**, *8*, 189–193.
- [13] a) J. S. Dewar, *Bull. Soc. Chim. Fr.* **1951**, *18*, C71–C79; b) J. Chatt, L. A. Duncanson, *J. Chem. Soc.* **1953**, 2939–2947.
- [14] W. P. Fehlhammer, M. Fritz, *Chem. Rev.* **1993**, *93*, 1243–1280.
- [15] a) U. Schlickum, R. Decker, F. Klappenberger, G. Zoppellaro, S. Klyatskaya, W. Auwärter, S. Neppel, K. Kern, H. Brune, M. Ruben, J. V. Barth, *J. Am. Chem. Soc.* **2008**, *130*, 11778–11782; b) F. Klappenberger, D. Kühne, W. Krenner, I. Silanes, A.

- Arnau, F. J. Garcia de Abajo, S. Klyatskaya, M. Ruben, J. V. Barth, *Nano Lett.* **2009**, *9*, 3509–3514; c) D. Kühne, F. Klappenberger, R. Decker, U. Schlickum, H. Brune, S. Klyatskaya, M. Ruben, J. V. Barth, *J. Phys. Chem. C* **2009**, *113*, 17851–17859; d) F. Klappenberger, D. Kühne, M. Marschall, S. Neppl, W. Krenner, A. Nefedov, T. Strunskus, K. Fink, C. Wöll, S. Klyatskaya, O. Fuhr, M. Ruben, J. V. Barth, *Adv. Funct. Mater.* **2011**, *21*, 1631–1642; e) E. Arras, A. P. Seitsonen, F. Klappenberger, J. V. Barth, *Phys. Chem. Chem. Phys.* **2012**, *14*, 15995–16001.
- [16] a) T. Yokoyama, S. Yokoyama, T. Kamikado, Y. Okuno, S. Mashiko, *Nature* **2001**, *413*, 619–621; b) Y. Okuno, T. Yokoyama, S. Yokoyama, T. Kamikado, S. Mashiko, *J. Am. Chem. Soc.* **2002**, *124*, 7218–7225; c) E. Y. Vedmedenko, N. Mikuszeit, *ChemPhysChem* **2008**, *9*, 1222–1240.
- [17] N. Henningsen, R. Rurali, C. Limbach, R. Drost, J. I. Pascual, K. J. Franke, *J. Phys. Chem. Lett.* **2011**, *2*, 55–61.
- [18] a) C. S. Kley, J. Cechal, T. Kumagai, F. Schramm, M. Ruben, S. Stepanow, K. Kern, *J. Am. Chem. Soc.* **2012**, *134*, 6072–6075; b) J. Cechal, C. S. Kley, T. Kumagai, F. Schramm, M. Ruben, S. Stepanow, K. Kern, *Chem. Commun.* **2014**, *50*, 9973–9976.
- [19] a) K. P. C. Vollhardt, *Angew. Chem. Int. Ed. Engl.* **1984**, *23*, 539–556; *Angew. Chem.* **1984**, *96*, 525–541; b) J. H. Hardesty, J. B. Koerner, T. A. Albright, G. Y. Lee, *J. Am. Chem. Soc.* **1999**, *121*, 6055–6067.
- [20] U. W. Hamm, V. Lazarescu, D. M. Kolb, *J. Chem. Soc. Faraday Trans.* **1996**, *92*, 3785–3790.
- [21] a) P. Magnus, L. M. Principe, *Tetrahedron Lett.* **1985**, *26*, 4851–4854; b) P. J. Low, R. Rousseau, P. Lam, K. A. Udachin, G. D. Enright, J. S. Tse, D. D. M. Wayner, A. J. Carty, *Organometallics* **1999**, *18*, 3885–3897; c) P. Magnus, C. Exon, P. Albaughrobertson, *Tetrahedron* **1985**, *41*, 5861–5869.
- [22] a) K. Gao, P. S. Lee, T. Fujita, N. Yoshikai, *J. Am. Chem. Soc.* **2010**, *132*, 12249–12251; b) P. S. Lee, T. Fujita, N. Yoshikai, *J. Am. Chem. Soc.* **2011**, *133*, 17283–17295.
- [23] N. E. Schore, *Chem. Rev.* **1988**, *88*, 1081–1119.
- [24] T. Kauffmann, *Angew. Chem. Int. Ed. Engl.* **1996**, *35*, 386–403; *Angew. Chem.* **1996**, *108*, 401–418.
- [25] J. H. Hall, R. L. Delavega, W. L. Purcell, *Inorg. Chim. Acta* **1985**, *102*, 157–162.
- [26] B. Fang, W. S. Ren, G. H. Hou, G. F. Zi, D. C. Fang, L. Maron, M. D. Walter, *J. Am. Chem. Soc.* **2014**, *136*, 17249–17261.
- [27] a) Y.-Q. Zhang, N. Kepčija, M. Kleinschrodt, K. Diller, S. Fischer, A. C. Papageorgiou, F. Allegritti, J. Björk, S. Klyatskaya, F. Klappenberger, M. Ruben, J. V. Barth, *Nat. Commun.* **2012**, *3*, 1286; b) H. Y. Gao, H. Wagner, D. Y. Zhong, J. H. Franke, A. Studer, H. Fuchs, *Angew. Chem. Int. Ed.* **2013**, *52*, 4024–4028; *Angew. Chem.* **2013**, *125*, 4116–4120; c) F. Bebensee, C. Bombis, S. R. Vadapoo, J. R. Cramer, F. Besenbacher, K. V. Gothelf, T. R. Linderoth, *J. Am. Chem. Soc.* **2013**, *135*, 2136–2139; d) O. Díaz Arado, H. Mönig, H. Wagner, J.-H. Franke, G. Langewisch, P. A. Held, A. Studer, H. Fuchs, *ACS Nano* **2013**, *7*, 8509–8515; e) J. Eichhorn, W. M. Heckl, M. Lackinger, *Chem. Commun.* **2013**, *49*, 2900–2902; f) J. Liu, P. Ruffieux, X. L. Feng, K. Müllen, R. Fasel, *Chem. Commun.* **2014**, *50*, 11200–11203; g) B. Cirera, Y.-Q. Zhang, J. Björk, S. Klyatskaya, Z. Chen, M. Ruben, J. V. Barth, F. Klappenberger, *Nano Lett.* **2014**, *14*, 1891–1897; h) F. Klappenberger, Y. Zhang, J. Björk, S. Klyatskaya, M. Ruben, J. V. Barth, *Acc. Chem. Res.* **2015**, *48*, 2140–2150.

Received: January 19, 2016  
Published online: April 6, 2016